

LEAD-FREE SOLDER DATA: COLLECTION AND DEVELOPMENT*

Thomas A. Siewert¹, David R. Smith¹, Yi-Wen Cheng¹, Juan-Carlos Madeni², and Steven Liu²

¹National Institute of Standards and Technology, Materials Reliability Division, Boulder, CO 80305, USA, ²Colorado School of Mines, Golden, CO 80401, USA,
siewert@boulder.nist.gov

ABSTRACT

The rising interest in lead-free solders creates a need for complete property data on the various lead-free solder compositions. Various types of data are available, but are widely dispersed through the literature. To improve the sharing of this important information, we developed an on-line database for solder properties emphasizing new lead-free solders.

As data came in, we found it difficult to combine data from some sources, due to differences in procedures under which the data were developed. Therefore, we developed a practice guide to offer some standard procedures for future work.

Finally, once we had collected as much information as possible, we began to develop data to fill in some of the gaps. Intermetallic formation and growth were studied for the alloys Sn-3.2Ag-0.8Cu, Sn-3.5Ag, Sn-0.7Cu, and Sn-9Zn. Coupons of solder joints (prepared by melting some of each solder alloy on a copper-plated circuit board) were subjected to thermal aging tests for 20, 100, 200, and 500 hours at 70, 100, and 150 °C. The results confirm that the formation of intermetallic layers is controlled by diffusion and that the intermetallic layers grow by thermal activation in a parabolic manner.

KEY WORDS

copper; intermetallics; lead-free solders; silver; solder; tin

INTRODUCTION

The worldwide "green" movement in the electronics industry to replace lead-tin eutectic solders with lead-free solders creates a need for critical data on the industry's new lead-free solder compositions for use in design and reliability models. Lead-free solder alloys cannot be simply substituted for conventional lead-containing alloys because of differences in their mechanical and physical properties. To use the new lead-free alloys in reliable and enduring products, accurate data must be inserted into the finite-element models of board designs.

Data on the various lead-free solder alloys are being developed rapidly, but are widely dispersed through the literature. We decided that it would be helpful to collect information on the most popular alloys, and make it widely available. Thus we developed an on-line database for solder properties emphasizing new lead-free solders. The site can be found at <http://www.boulder.nist.gov/div853/lead%20free/solders.html>.

*Contribution of NIST; not subject to copyright in the U.S.

When the data from different sources were combined, it was found to contain more variation than was expected. We attributed much of this to differences in procedures under which the data were developed. Therefore, we worked with the solder experts on a NEMI (National Electronics Manufacturing Initiative) committee to develop a practice guide with some standardized procedures. This guide can be downloaded from http://www.boulder.nist.gov/div853/Program3_solder.htm.

Once we had collected as much information as possible from the literature and from researchers, we began to develop data to fill in some of the gaps. We decided to compare four of the lead-free solders that have been shown to be promising in studies by the National Center for Manufacturing Sciences (NCMS), and by NEMI [1-2]. These were the alloys Sn-3.2Ag-0.8Cu, Sn-3.5Ag, Sn-0.7Cu, and Sn-9Zn.

The formation of intermetallic phases in an electronic joint is usually disadvantageous because the intermetallic phases are typically brittle and may be more susceptible to crack growth. However, the intermetallic compounds are an indication of chemical bonding at the substrate/solder interface [3], so small amounts of intermetallic compounds can be considered to indicate that the soldering process has formed a good bond. In some cases, small amounts of intermetallic compounds can even produce some improvements in the mechanical and thermal properties of solder joints, and promote wetting and bonding processes [4]. According to Harris and Chaggar [5], the presence of the intermetallics Ag_3Sn and Cu_6Sn_5 in the tin solid solution in the alloys Sn-3.5Ag and Sn-0.7Cu respectively, improves hardness and resistance to fatigue. However, the negative effects tend to dominate. Their hardness is usually several times greater than that of either the copper or the tin, and their resistivity is usually many times greater than that of the copper. In any case, it is almost impossible to avoid the formation of intermetallics, so their presence (and their properties) must be factored into designs.

The intermetallic phases are products of the solder-substrate interactions. An initial layer forms during the soldering process, and continues to grow in the solid state, especially at elevated temperatures. The growth of the intermetallic layer follows a parabolic growth curve, as expressed by equation (1):

$$X = (kt)^{1/2}, \quad (1)$$

where X is the thickness of the intermetallic layer, t is the time, and k is the growth constant at a specific temperature.

This mechanism assumes that the growth of the intermetallic compound layer is controlled by bulk diffusion of reactants to the reaction interface. The parabolic reduction in growth rate with time reflects the increase in the diffusion path as the already formed intermetallic layers impede the transport of additional reactants. In some cases, multiple intermetallics, such as both Cu_3Sn and Cu_6Sn_5 , can form between copper and tin.

PROCEDURES

The solder alloys were deposited on coupons cut from an FR4 PCB, which had been plated with about 45 or 50 μm of copper [6]. The coupons were about 25 mm square. After a protective coating was removed from the copper surface, the coupons were cleaned by rinsing with ethanol, then a water-based solution of ammonium hydroxide, trisodium phosphate, and sodium tetraborate pentahydrate. After the copper surfaces dried (a few seconds), a solution of water-based phosphoric acid was applied (for the silver- and copper-bearing alloys). Next, the three molten solders, at 50 °C above their melting temperatures, were deposited on the substrates and the coupons were cooled in air to ambient temperature. In the case of alloy Sn-9Zn, the copper surface was prepared by use of commercial zinc chloride- and ammonium chloride-based paste. The cleaning agent was applied on the copper surface just before the molten solder alloy was deposited on it, and provided better wetting than the phosphoric acid solution chosen for the other three solder alloys.

The copper/solder coupons were thermally aged in a furnace that was accurate and uniform to within ± 1 °C. To avoid oxidation during thermal aging, industrial-grade argon gas was fed to the furnace. The specimens were aged according to a 3-by-4 matrix design (temperatures 70, 100 and 150 °C, for 20, 100, 200 and 500 hours). The furnace was open for only a short time (< 2 seconds) as the specimens were extracted, which had an insignificant effect on the temperature. The specimens were water-quenched as they were removed from the furnace.

After thermal aging, the specimens were cut in half, perpendicular to the flat surface of the copper substrate, and cold-mounted in epoxy to display the cross-section for metallographic analysis. Using standard metallographic techniques, the mounted specimens were ground and polished with a 0.5 μm diamond slurry, followed by vibratory polishing for 40 minutes in an aqueous solution of colloidal silica. The final finish was quite satisfactory for resolving the intermetallic compounds at the copper/solder interface. The copper/solder interfaces of the specimens were examined by light microscopy to differentiate the intermetallic layers, by scanning electron microscopy (SEM) to obtain backscattered electron images (BEI) that contrasted the chemical composition differences between different phases, and by energy dispersive spectroscopy (EDS) for element identification. Quantitative measurements of the thickness of the intermetallic layers were made using a digital image analysis system. To obtain an accurate average thickness for the very uneven interfaces, between 20 and 40 measurements were taken at the interface on each specimen. The intermetallic compounds (IMCs) were identified by EDS. After centering the electron beam on the area of interest, the spectrum was acquired and an approximate composition was calculated.

RESULTS AND DISCUSSION

A typical copper-solder interface, after soldering but before thermal aging, is shown in Figure 1. The most noticeable features of the structure (from bottom to top) are the circuit-board substrate, the copper pad, and the solder. Only at high magnifications can very small amounts of Cu_6Sn_5 be resolved at the copper/solder interface [7]. Note that the copper/solder interface is not perfectly planar. In fact, the copper boundary has a very irregular shape.

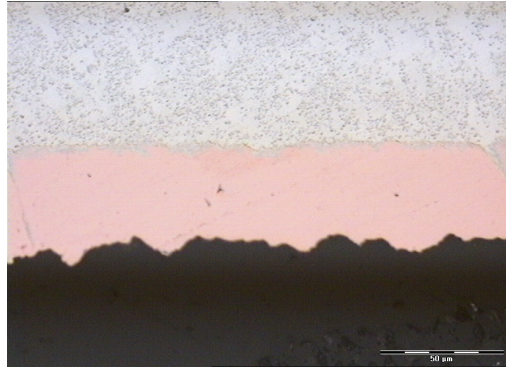


Figure 1. Copper/Sn-3.5Ag solder interface prior to thermal aging.

The thermal aging changed the microstructure at the copper/solder interface as the intermetallic layers grew. After only 20 hours, a very thin dark line of Cu_6Sn_5 was visible at the copper/Sn-3.5Ag interface, even at this relatively low magnification of 600 X. As the aging time increased, the IMC layer grew, but more slowly. The specimens exposed for 100, 200, and 500 hours display two distinct intermetallic layers, Cu_3Sn and Cu_6Sn_5 . A similar trend is observed in the other systems (Cu/Sn-3.2Ag-0.8Cu, Cu/Sn-0.7Ag and Cu/Sn-9Zn). However, in the case of the Cu/Sn-9Zn interface, only one intermetallic phase is observed, Cu_5Zn_8 . The thicknesses of the layers of these intermetallic compounds varied with the solder system.

Thermodynamic calculations predict the formation of Cu_5Zn_8 in the Sn-9Zn alloy, instead of the Cu_3Sn and Cu_5Sn_6 intermetallic compounds usually found in tin-rich alloys. The free-energy change of the reactions (-7.8 kJ/mol for Cu_3Sn , -7.4 kJ/mol for Cu_5Sn_6 and -12.3 kJ/mol for Cu_5Zn_8) calculated by use of the Gibbs-Helmholtz equation, clearly indicate that Cu_5Zn_8 is the most likely to form.

The kinetics of the IMC growth was determined as a function of aging time and temperature for both individual Cu_3Sn and Cu_6Sn_5 layers and the combined ($\text{Cu}_3\text{Sn} + \text{Cu}_6\text{Sn}_5$) IMC thicknesses. The mean values of the total intermetallic layer thicknesses at the greatest growth condition, 150 °C for 500 hours, in the four copper-solder systems were found to be: 13 μm for Cu/Sn-3.5Ag, 14 μm for Cu/Sn-3.2Ag-0.8Cu, 14 μm for Cu/Sn-0.7 Cu, and 19 μm for the Cu/Sn-9Zn alloy.

The observed total IMC thickness and time relationships at 70, 100 and 150 °C, are shown in Figures 2 (a), (b), and (c). They all obey the predicted parabolic relationship. The slopes of the lines in Figure 2 indicate the rate of IMC growth. As expected, as the temperature increased, the rate of IMC layer growth increased. At all three temperatures, the intermetallic in Sn-9Zn grows distinctly faster than that of the others alloys, which are fairly tightly grouped. At 70 and 100 °C, the intermetallic in Sn-3.5Ag grows at a slightly slower rate, while at 150 °C, the intermetallic in Sn-3.2Ag-0.8Cu grows at the slowest rate.

Similar analyses were done with the individual IMCs in each copper/solder system. The general observation is that their growth also obeys the parabolic relation, as in the case of the growth of the total IMC. The following observations on the individual layers are based on

analysis of the mean values, but some of the scatter bands are fairly wide (as shown by the vertical bars), compared to the differences between the means, so some of these trends are weak.

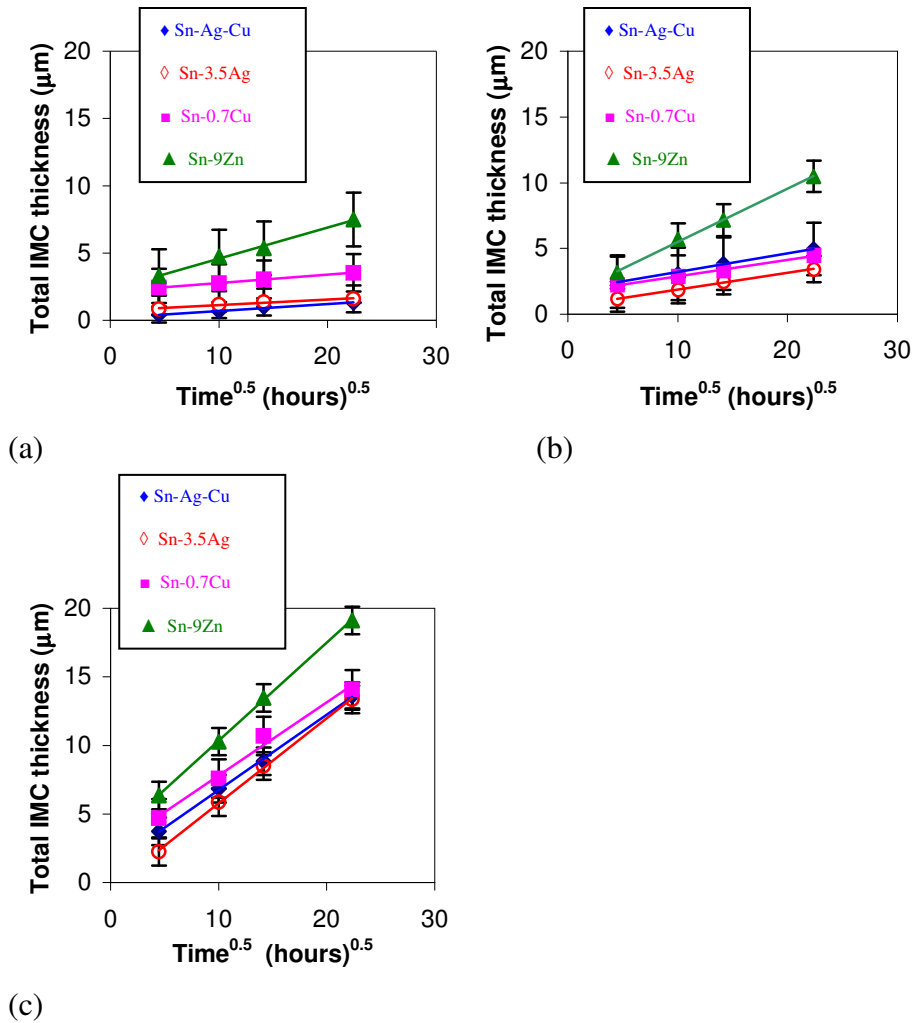


Figure 2. Total IMC growth ($\text{Cu}_3\text{Sn} + \text{Cu}_6\text{Sn}_5$) at the copper/solder interface at three temperatures, (a) 70 °C, (b) 100 °C, and (c) 150 °C. In each case, the bars show the range in thickness measurements (from between 20 and 40 individual measurements for each specimen), and the symbol is at the mean.

In the case of the Cu/Sn-3.2Ag-0.8Cu joint system, shown in Figure 3 (a), the initial thicknesses and the growth rates for the two intermetallics are very similar. From the slight difference in the slopes of the means, we might conclude that the Cu_6Sn_5 intermetallic grows at a slightly faster rate than the Cu_3Sn .

For the Cu/Sn-3.5Ag system, shown in Figure 3 (b), one sees that the Cu_6Sn_5 and Cu_3Sn layers start at almost the same thickness. By 150 hours, the thickness of Cu_3Sn is distinctly less, so its growth rate is slower. Perhaps this difference in behavior from that of the

previous alloy is due to a larger fraction of tin is reacting with silver to form Ag_3Sn at the Cu_6Sn_5 growth front.

In the case of the Cu/Sn -0.7Cu system, shown in Figure 3 (c), Cu_3Sn starts with a thicker layer, but grows at approximately the same rate as Cu_6Sn_5 . The Cu_3Sn layer may grow faster here than for the previous two alloys because no Ag_3Sn is formed in this system, so more tin atoms can migrate through the Cu_6Sn_5 layer to form Cu_3Sn .

In the case of the Cu/Sn -9Zn system, only Cu_5Zn_8 forms. Figure 3 (d) shows that its growth is faster than for the sum of both of the intermetallics in the other alloys.

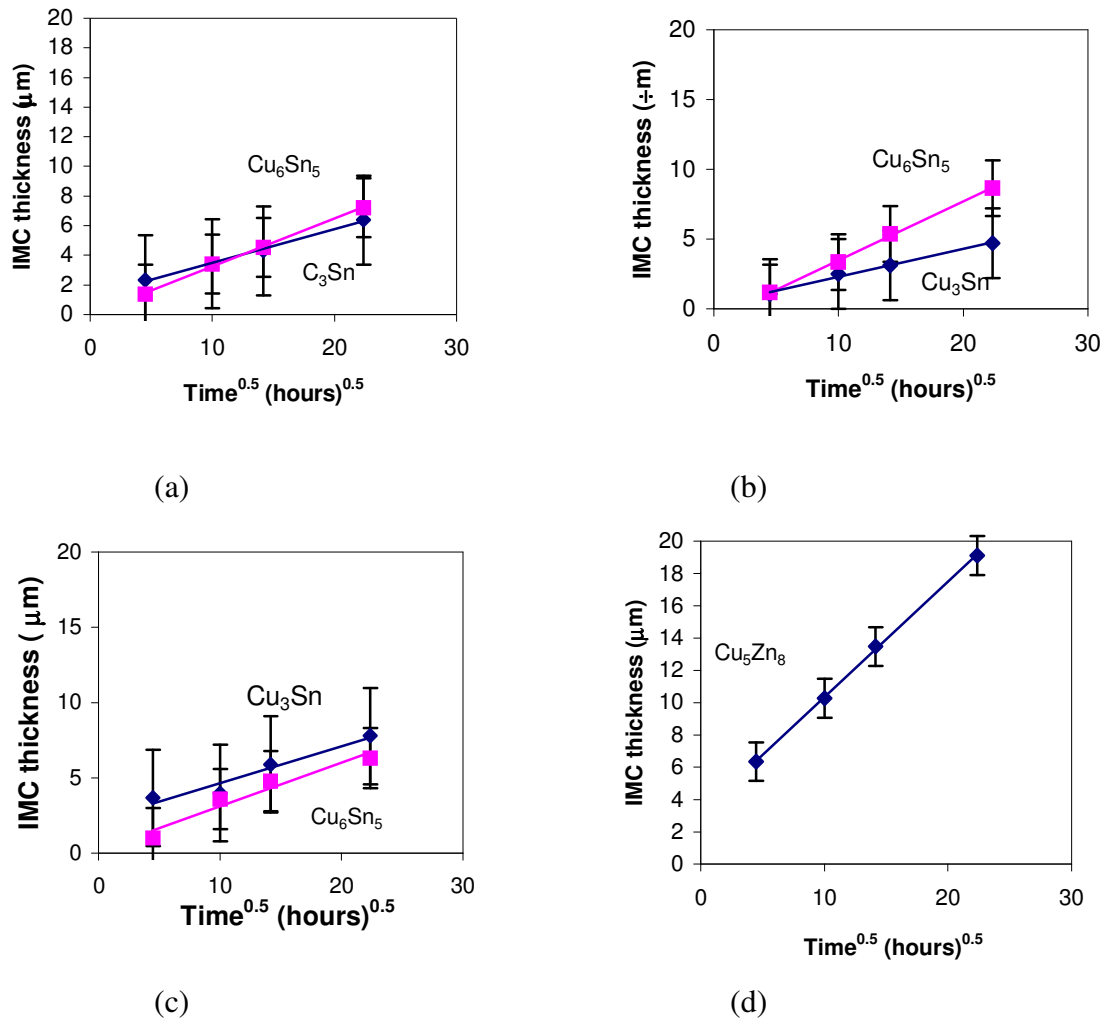


Figure 3. Individual intermetallic component layers growth for specimens aged at 150 °C, (a) Sn-3.2Ag-0.8Cu, (b) Sn-3.5Ag, (c) Sn-0.7Cu, and (d) Sn-9Zn. In the first three plots, Cu_3Sn is identified by the diamonds and Cu_6Sn_5 by the squares.

The constant k in equation (1) is determined from the slopes of the lines in the IMC thickness as a function of log time plots. After adding the temperature dependence and normalizing the equation to a linear form using a regression model, the $\log k$ can be determined as a function of $(1/T)$ plots for the individual phases and for the total IMC. Figures 4 through 7 display these plots for each alloy system. The constant k_0 is expressed in units of [micrometers*hour^{-1/2}], with the gas constant, R , equal to 8,314 J/(mol·K), implying that the temperature must be in kelvins. Using these units, the activation energy, Q , is determined in units of J/mol. The activation energy, Q , is calculated from the slope ($s = -Q/2.3R$) of the $\log k$ versus $1/T$ plots.

Both Figures 4 (a) and (b) are for the Cu/Sn-3.2Ag-0.8Cu system. The slopes of the lines in Figure 4 (a) suggest similar activation energies for the two intermetallic compounds. Since the slope of the line in Figure 4 (b) is almost the same as those of the individual IMCs, the activation energy for the total IMC will be very close to those of the individual IMCs.

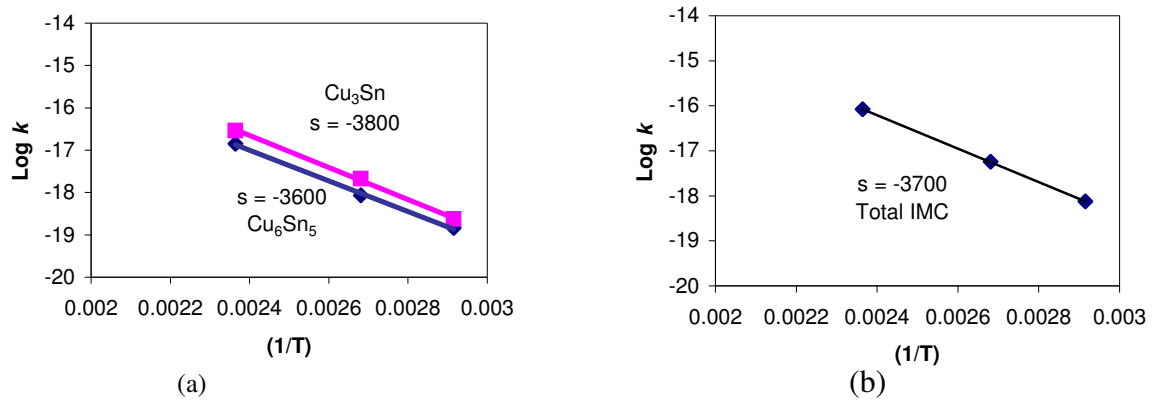
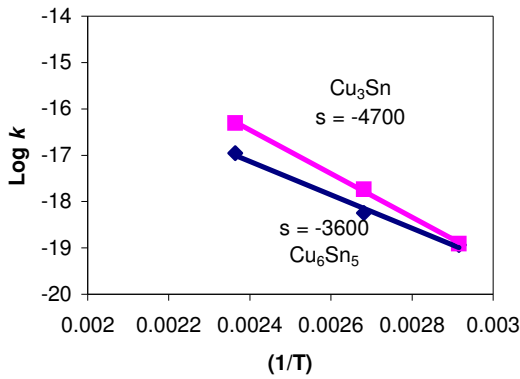
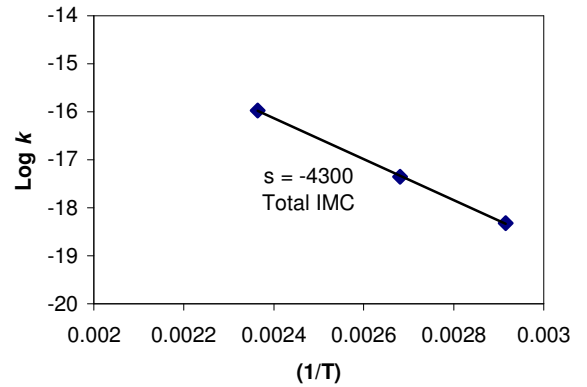


Figure 4. $\log k$ as a function of $(1/T)$ for (a) individual IMCs (Cu_3Sn and Cu_6Sn_5), (b) total IMC ($\text{Cu}_3\text{Sn} + \text{Cu}_6\text{Sn}_5$) in the Cu/Sn-3.2Ag-0.8Cu system. In Figure 4 (a), the squares represent the Cu_3Sn data.

The plots in Figures 5 (a) and (b) are for the Cu/Sn-3.5Ag system. The slopes of the lines in Figure 5 (a) suggest a higher activation energy for the Cu_6Sn_5 formation than for Cu_3Sn . The line on Figure 5 (b) corresponds to the combination of the two intermetallic phases in one layer. As expected, its slope suggests an intermediate value for the activation energy.

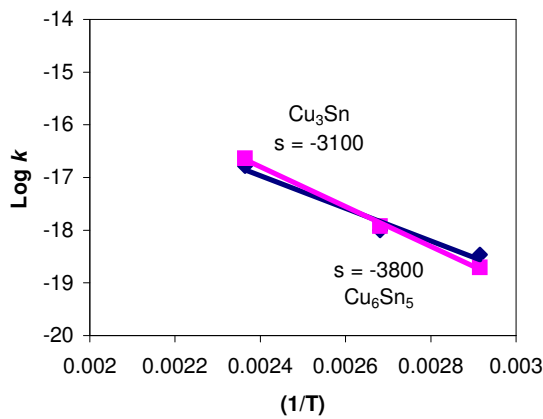


(a)

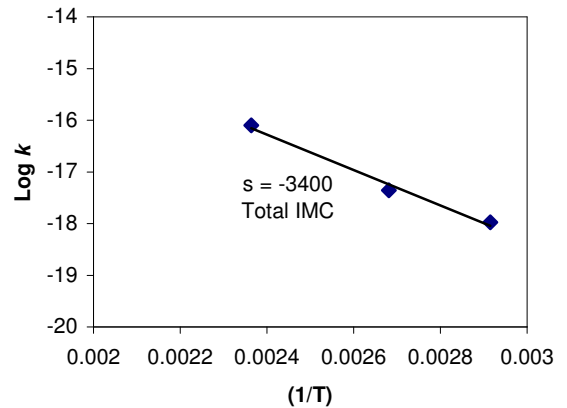


(b)

Figure 5. Log k as a function of $(1/T)$ for (a) individual IMCs (Cu_3Sn and Cu_6Sn_5), (b) total IMC ($\text{Cu}_3\text{Sn} + \text{Cu}_6\text{Sn}_5$) in the Cu/Sn-3.5Ag system. In Figure 5 (a), the squares represent the Cu_3Sn data.



(a)



(b)

Figure 6. Log k as a function of $(1/T)$ for (a) individual IMCs (Cu_3Sn and Cu_6Sn_5), (b) total IMC ($\text{Cu}_3\text{Sn} + \text{Cu}_6\text{Sn}_5$) in the Cu/Sn-0.7Cu system. In Figure 6 (a), the squares represent the Cu_3Sn data.

The plots for the Cu/Sn-0.7Cu system are exhibited in Figures 6 (a) and (b). The slope of the Cu_6Sn_5 line indicates an activation energy higher than that of the Cu_3Sn . The intersection of the two lines in Figure 6 (a) indicates that at high temperatures the rate of formation of Cu_6Sn_5 is higher than that of Cu_3Sn ; at low temperatures the opposite occurs. The slope of the line on Figure 6 (b), which is for the total IMC thickness ($\text{Cu}_3\text{Sn} + \text{Cu}_6\text{Sn}_5$), indicates an intermediate value for the activation energy.

In the case of the Cu/Sn-9Zn system, a single activation energy is determined. Since the slope of the line in Figure 7 is the smallest among the four copper/solder systems, the smallest value of activation energy is observed.

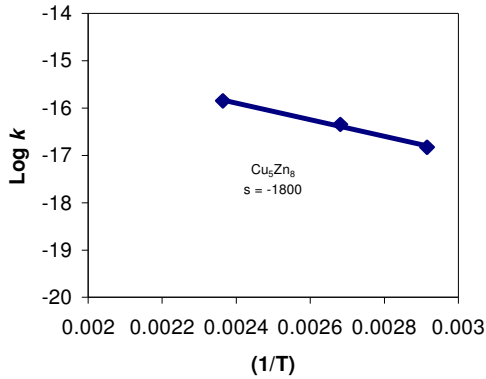


Figure 7. Log k as a function of (1/T) for the total IMC in the Cu/Sn-9Zn system (in this system there is only one IMC).

As the activation energy of a specific intermetallic compound increases, the formation and growth of this compound becomes more difficult. On the other hand, low activation energies indicate easier formation and growth of IMCs. The calculated activation energies represent both the formation and motion of vacancies responsible for the interfacial reaction. Q , the activation energy, is stated in the following equation:

$$Q = \Delta H_m + \Delta H_f, \quad (2)$$

where ΔH_f is the enthalpy change needed to form a mole of vacancies and ΔH_m is the enthalpy change or energy barrier that must be overcome to move a mole of atoms into vacancies.

The activation energies for the total IMC thickness and for the individual phases for the four solder alloys are presented in Table 1. The activation energy data for the Cu/Sn-3.5Ag and Cu/Sn-0.7Cu joint systems agree well with previous studies found in the literature [8, 9]. In the case of the Cu/Sn-3.2Ag-0.8Cu and Cu/Sn-9Zn joint systems, no comparative data were found.

Table 1. Activation energies, Q, derived from the data for the total and individual IMCs in the Cu/Sn-3.2Ag-0.8Cu, Cu/Sn-3.5Ag, Cu/Sn-0.7Cu, and Cu/Sn-9Zn joint systems.

ALLOY	IMC	Q (kJ/mol)	Q (eV/atom)
Sn-3.2Ag-0.8Cu	Total	70	0.74
	Cu ₃ Sn	69	0.72
	Cu ₆ Sn ₅	72	0.75
Sn-3.5Ag	Total	82	0.85
	Cu ₃ Sn	69	0.72
	Cu ₆ Sn ₅	90	0.93
Sn-0.7Cu	Total	66	0.68
	Cu ₃ Sn	59	0.61
	Cu ₆ Sn ₅	72	0.75
Sn-9Zn	Cu ₅ Zn ₈	34	0.35

CONCLUSIONS

- Three intermetallic compounds were found at the Cu/Sn-3.5Ag and Cu/Sn-3.2Ag-0.8Cu interfaces: Cu₃Sn, Cu₆Sn₅ and Ag₃Sn.
- At the Cu/Sn-0.7Cu interface, two IMC layers were found: Cu₃Sn and Cu₆Sn₅.
- At the Cu/Sn-9Zn interface, only Cu₅Zn₈ was found.
- The intermetallic layers grow by thermal activation in a parabolic manner.
- The IMCs, Cu₃Sn, Cu₆Sn₅ and Cu₅Zn₈, formed layers of uneven thickness and grew at different rates, depending on the alloy composition.
- If minimizing IMC growth is the major criterion, Sn-3.5Ag seems to be the best solder material for electronic soldering because the IMC at the Cu/Sn-3.5Ag interface grows more slowly than in the other three systems.
- The solder alloy Sn-9Zn had the fastest IMC growth.
- The other two alloys, Sn-3.2Ag-0.8Cu and Sn-0.7Cu, had growth rates that were intermediate, but close to that of Sn-3.5Ag.

REFERENCES

1. National Center for Manufacturing Sciences (NCMS), "The Lead-free Solder Project", NCMS Report 0401RE96, (1997).
2. "Roadmap of Lead-Free Assembly in North America," JISSO/PROTEC Forum 2002, November 19-20, 2002; Japan.
3. Shan-Pu Yu, Moo-Chin Wan, Min-Hsiung Hon, "Formation of Intermetallic Compounds at Eutectic Sn-Zn-Al Solder/Cu Interface", J. Mater. Res., Vol. 16, No. 1, Jan (2001).
4. Y. G. Lee, J. G. Duh, "Characterizing the Formation and Growth of Intermetallic Compounds in the Solder Joint", Journal of Material Science, 33, (1998), pp. 5569-5572.
5. Paul G. Harris, Kaldev S. Chaggar, "The Role of Intermetallic Compounds in Lead-free Soldering" Soldering and Surface Mount Technology, 10/3, (1998), pp. 38-52.

6. J. Madeni, S. Liu, and T. Siewert, "Intermetallics Formation and Growth at the Interface of Tin-based Solder Alloys and Copper Substrates", 2nd International Brazing and Soldering Conference, February 17-19, San Diego, California.
7. A. Zibri, A. Clark, L. Zavalij, P. Borgesen, and E. J. Cotts, "The Growth of Intermetallic Compounds at Sn-Ag-Cu Solder/Cu and Sn-Ag-Cu/Ni Interfaces and the Associated Evolution of the Solder Microstructure", JOM, Vol. 30, No. 6, (2001), pp. 1157-1164.
8. P. T. Vianco, A. C. Kilgo, R. Grant, "Intermetallic Compound Layer Growth Kinetics in Non Lead Bearing Solders", Sandia National Laboratories, Albuquerque, NM, (1995).
9. D. R. Flanders, E. G. Jacobs and R. F. Pinizzotto, "Activation Energies of Intermetallic Growth of Sn-Ag Eutectic Solder on Copper Substrates", JOM, Vol. 26, No. 7, (1997).